Journal of Physics: Conference Series

PAPER • **OPEN ACCESS**

Classical and quantum warm dense electron gas dynamic characteristics: analytic predictions

To cite this article: J. Ara *et al* 2022 *J. Phys.: Conf. Ser.* **2270** 012041

View the article online for updates and enhancements.

ECS Membership = Connection

ECS membership connects you to the electrochemical community:

- Facilitate your research and discovery through ECS meetings which convene scientists from around the world;
- Access professional support through your lifetime career:
- Open up mentorship opportunities across the stages of your career;
- Build relationships that nurture partnership, teamwork—and success!

Join ECS! Visit electrochem.org/join

ECS

This content was downloaded from IP address 158.42.140.65 on 31/05/2022 at 11:39

Classical and quantum warm dense electron gas dynamic characteristics: analytic predictions

J. Ara[1], A.V. Filinov[2], I.M. Tkachenko[3,4]

[1] Instituto de Tecnología Química, Universitat Politècnica de València-Consejo Superior de Investigaciones Científicas, Valencia, Spain
[2] Institut für Theoretische Physik und Astrophysik, Christian-Albrechts-Universität zu Kiel, Germany
[3] Departament de Matemàtica Aplicada, Universitat Polièchica de València, Valencia, Spain
[4] Al-Farabi Kazakh National University, Almaty, Kazakhstan

E-mail: imtk@mat.upv.es

Abstract.

We apply a novel 9-moment variational version of the self-consistent non-perturbative method of moments to study how the temperature affects the dynamic response of the electron gas in thermodynamic equilibrium. The theoretical results are obtained with the only input being the static structure factor. Comparison is carried out with the data obtained in the random-phase and the effective static local-field (ESA) (1) approximations. A quite satisfactory agreement is achieved with the system dynamic structure factor evaluated within the ESA interpolation scheme. We analyze the system properties for the temperature values ($1 \leq T/T_F \leq 4$) chosen in the range where the electron gas starts to undergo a transition from the degenerate to classical behaviour. The extension of the method to a broader range of temperatures and densities is straightforward and is left for future studies. Nevertheless, we demonstrate a systematic way to investigate the gradual transition from degenerate to classical systems.

1. Introduction

A warm dense gas of electrons (see (2) and references therein) is an important particular case of one-component fluids of charged particles and a key-model for a broad class of warm dense matter systems which (i) is widely used to testify different theoretical approaches, and (ii) is of significant practical importance for the interpretation and development of real experimental studies. Development of novel theoretical simulation techniques for warm dense matter is also of utmost interest and importance.

Until recently only *ab initio* path-integral Monte-Carlo (PIMC) simulation results on different characteristics of a dense warm uniform electron gas (UEG) (see (3) and references therein) were available. As any simulation data, these results are available in a limited realm of physical parameters, e.g. the smallest wavenumber being accessible is specified by the system size, $k = 2\pi/L$. Lately, we have presented (4; 5; 6) preliminary theoretical results on the static and dynamic properties of the UEG obtained within the self-consistent approach based on the non-perturbative method of moments capable of expressing the system (inverse) dielectric function, $\epsilon^{-1}(q,\omega)$, its static value, the dynamic structure factor, $S(q,\omega)$, and other dynamic characteristics exclusively in terms of the UEG static structure factor (SSF), $S(q)$, and using

Content from this work may be used under the terms of the Creative Commons Attribution 3.0 licence. Any further distribution of this work must maintain attribution to the author(s) and the title of the work, journal citation and DOI.
Published under licence by IOP Publishing Ltd

up to nine sum rules and other exact properties (7; 8; 5). The input SSF has been taken from the recent PIMC simulations (9) by T. Dornheim, S. Groth and M. Bonitz. The obtained interrelations produce results which are in a good agreement with the available PIMC data (3).

In the present work, we extend the self-consistent method of moments (SCMM) onto a broader domain of thermodynamic parameters (r_s, θ) and wavenumbers (k/k_F), and focus on the analysis of dynamic characteristics vs. the degeneracy (controlled by the temperature).

2. Parameters and sum rules

The thermodynamic state of the UEG can be uniquely specified by the standard coupling and degeneracy parameters ($\{\Gamma, D\}$ or $\{r_s, \theta\}$)

$$\Gamma = \beta e^2/a = \beta e^2 \sqrt[3]{4\pi n/3} \ , \quad D = \beta E_F = \theta^{-1} \ , \quad r_s = 1.842\Gamma\theta \ , \tag{1}$$

where β is the inverse temperature, n is the number density, and a is the average interparticle spacing. In the following analysis we will consider the warm dense matter regime (10) with $r_s, \theta \sim 1$. Nevertheless, the approach we suggest is non-perturbative so that the region of parameter values can be extended as soon as new simulation data (on the SSF) become available. The wavenumber-dependence will be expressed via the dimensionless parameter $q = ka$ or k/k_F.

In the linear response regime, the loss function (or the spectral density) is the central quantity for modeling of the inverse dielectric function $\epsilon^{-1}(q,\omega)$ and the dynamic structure factor $S(q,\omega)$

$$\mathcal{L}(q,\omega) = -\mathrm{Im}\,\epsilon^{-1}(q,\omega)/\pi\omega, \quad S(q,\omega) = \frac{q^2 n}{3\pi\Gamma}\beta\hbar\omega(1-\exp(-\beta\hbar\omega))^{-1}\mathcal{L}(q,\omega). \tag{2}$$

The method of moments is based on a direct relation between the above dynamical properties and the sum rules introduced as the loss function frequency power moments

$$C_\ell(q) = \int_{-\infty}^{\infty} \omega^\ell \, \mathcal{L}(q,\omega)\, \mathrm{d}\omega \ , \quad \ell = 0, 1, 2, ...8, \tag{3}$$

or the characteristic frequencies

$$\omega_j(q) = \sqrt{C_{2j}/C_{2j-2}(q)} \ , \quad j = 1, 2, 3, 4 \tag{4}$$

The odd-order moments vanish due to the symmetry of the loss function. The zero-th moment, due to the Kramers-Kronig relations, specifies the static limit of the inverse dielectric function, $C_0(q) = 1 - \epsilon^{-1}(q,0)$, and the plasma frequency enters in the f-sum rule, $C_2 = \omega_p^2$. The knowledge of the fourth moment, by virtue of the detailed balance condition (see (5) and references therein),

$$C_4(q) = \frac{6e^2}{aq^2\hbar n}\int_{-\infty}^{\infty}\omega^3 S(k,\omega)\, d\omega =$$

$$= \omega_p^4\left\{1 + \frac{q^2}{\Gamma}\theta^{3/2} I_{3/2}(\eta) + \frac{q^4}{12 r_s} + \frac{1}{3\pi}\int_0^\infty [S(p)-1]\, f(p,q)\, p^2 dp\right\} \ , \tag{5}$$

is reduced to the UEG static structure factor, $S(q)$. Here

$$f(p,q) = \frac{5}{6} - \frac{p^2}{2q^2} + \frac{\left(p^2-q^2\right)^2}{4q^3 p}\ln\left|\frac{q+p}{q-p}\right| \ , \tag{6}$$

and $I_{3/2}(\eta)$ is the Fermi integral, $I_{1/2}(\eta) = (2/3)/\sqrt{\theta^3}$ is the normalization condition. In a classical system the third term in (5) vanishes and the second contribution takes the Vlasov form, q^2/Γ.

3. The self-consistent solution of the five- and nine-moment problems

It was demonstrated in our previous works (7; 8) that the dynamic properties of classical Coulomb and Yukawa systems can be quite accurately described by the method of moments in the *five-moment approximation*. The corresponding Hamburger problem $\{C_0(q), 0, C_2, 0, C_4(q)\}$ and the Nevanlinna theorem (11; 12; 13) results in the following ansatz for the inverse dielectric function and the dynamic structure factor

$$\epsilon^{-1}(q,\omega;Q_2) = 1 + \frac{\omega_p^2\left(\omega + Q_2(q,\omega;\omega_1,\omega_2)\right)}{\omega\left(\omega^2-\omega_2^2(q)\right) + Q_2(q,\omega;\omega_1,\omega_2)\left(\omega^2-\omega_1^2(q)\right)}\ , \tag{7}$$

$$S(q,\omega) = \frac{q^2 n}{3\pi\Gamma}\left(\frac{\beta\hbar\omega}{1-\exp(-\beta\hbar\omega)}\right)\left(-\frac{\mathrm{Im}\epsilon^{-1}(q,\omega;Q_2)}{\omega}\right). \tag{8}$$

Both characteristics are determined by the frequencies $\omega_{1(2)}(q)$ and a non-phenomenological function $Q_2(q,\omega;\omega_1,\omega_2)$. The quantitative agreement with the OCP molecular-dynamics data (both on Coulomb and Yukawa systems) could be achieved (7; 8) even within the static approximation of the Nevanlinna (response) function $Q_2(q,z)$ such that $\lim_{z\to\infty}\left(Q_2(q,z)/z\right)$, $\mathrm{Im}z>0$ (14),

$$Q_2(q,z;\omega_1,\omega_2) = Q_2\left(q,0^+;\omega_1,\omega_2\right) = ih_2(q;\omega_1,\omega_2)\ . \tag{9}$$

The key physical assumption made and validated (7; 8) was that the zero-frequency Rayleigh mode is generally absent in the above classical systems. This permits to determine the static parameter as $h_2(q;\omega_1,\omega_2) = \omega_2^2(q)/\left(\sqrt{2}\omega_1(q)\right)$.

Such a relatively simple approach proves to be insufficient for quantum Fermi fluids of charged particles, as it is demonstrated in the analysis below (see Fig. 1 and the corresponding discussion). Our interpretation of this result is the existence in the spectrum of the second harmonic of the collective plasmon mode. Some indications of this mode, however, quite weak have been recently reported in (3).

The three-mode structure of the system spectrum can be adequately considered taking into account the sixth and the eighth moments or the frequencies $\omega_3(q)$ and $\omega_4(q)$. To this end we applied the nine-moment Nevanlinna formula (11; 12; 13), and equalized the five- and nine-moment expressions for the dielectric function. As a result the response-function $Q_2(q,z;\omega_1,\omega_2)$ introduced above is substituted with a new Nevanlinna parameter $Q_4(q,z;\omega_1,\omega_2,\omega_3,\omega_4)$. The absence of the zero-frequency Rayleigh mode (7) also in quantum fluids by the quantum-classical correspondence principle, allows us to employ the same static approximation to the function $Q_4(q,z;\omega_1,\omega_2,\omega_3,\omega_4)$ and find a new parameter $h_4(q;\omega_1,\omega_2,\omega_3,\omega_4)$. Thus we relate the dynamic five-moment Nevanlinna function,

$$\begin{aligned} Q_2(q,\omega;\omega_1,\omega_2,\omega_3,\omega_4) &= -\frac{\omega_2^2\left(\omega_3^2-\omega_2^2\right)}{\omega_2^2-\omega_1^2}\frac{(\omega+ih_4)}{\omega(\omega+ih_4)+\left(\frac{\omega_1^2\left(\omega_3^2-\omega_2^2\right)}{\left(\omega_2^2-\omega_1^2\right)}-\frac{\omega_3^2\left(\omega_4^2-\omega_3^2\right)}{\left(\omega_3^2-\omega_2^2\right)}\right)}\ , \\ h_4(q;\omega_1,\omega_2,\omega_3,\omega_4) &= \frac{\omega_3^2\left(\omega_4^2-\omega_3^2\right)\left(\omega_2^2-\omega_1^2\right)}{\omega_1\sqrt{2\left(\omega_3^2-\omega_1^2\right)\left(\omega_3^2-\omega_2^2\right)^3}}\ , \end{aligned} \tag{10}$$

to the new parameters $\omega_3(q)$ and $\omega_4(q)$. Certainly, the above expressions simplify into the *five-moment* case as soon as we consider two successive limiting transitions: $\omega_4(q)\to\infty$ and then $\omega_3(q)\to\infty$ (with $\omega_3(q)<\omega_4(q)$ following from the Cauchy-Schwarz-Bunyakovsky inequalities).

The characteristic frequency $\omega_1(q) = \omega_p\sqrt{1-\epsilon^{-1}(q,0)}$ and the static dielectric function were determined by direct analytical and numerical integration in the five- and nine-moment cases, respectively (5), without any significant difference being observed. The frequency $\omega_2(q)$ was determined by $S(q)$, see Eqs. (4),(5). Thus we reduced the knowledge of the dynamic structure factor, see Fig. 1, to that of the SSF.

4. The Shannon entropy maximization technique

The frequencies $\omega_3(q)$ and $\omega_4(q)$ formally introduced in terms of the higher-order moments, see Eq. (4), are determined by the virtually unknown three- and four-point static correlators. On the other hand, the frequencies $\omega_1(q)$ and $\omega_2(q)$ are uniquely determined by the SSF (5). Taking into account that the spectral density (here the loss function $\mathcal{L}(q,\omega)$) is formed by different combinations of quasi-particle excitations – the microstates in the sense of statistical ensemble, we decided that the optimal solution (most probable) should satisfy the principle of maximum entropy. This allows to determine the unknown parameters $\omega_{3(4)}$ by means of the Shannon information-entropy maximization procedure (15; 16; 17; 18), see also (13). Precisely, we suggest and resolve the maximization equations for the two-parameter Shannon entropy functional:

$$S(q;\omega_3,\omega_4) = -\int\limits_{-\infty}^{\infty} \mathcal{L}(\omega_3,\omega_4,q,\omega)\ln\left[\mathcal{L}(\omega_3,\omega_4,q,\omega)\right]\mathrm{d}\omega, \tag{11}$$

$$\begin{cases} -\int\limits_{-\infty}^{\infty}\left\{\frac{\partial\mathcal{L}(\omega_3,\omega_4;q,\omega)}{\partial\omega_3}\ln\left[\mathcal{L}(\omega_3,\omega_4;q,\omega)\right]\right\}d\omega = 0, \\ -\int\limits_{-\infty}^{\infty}\left\{\frac{\partial\mathcal{L}(\omega_3,\omega_4;q,\omega)}{\partial\omega_4}\ln\left[\mathcal{L}(\omega_3,\omega_4;q,\omega)\right]\right\}d\omega = 0. \end{cases} \tag{12}$$

The Hessian of the entropy (11) was studied to warrant its maximization at the solution of the system (12).

5. Numerical results

To validate our model solution with the higher order moments included (to allow for a second harmonic) and the principle of maximum entropy for the spectral density, we have performed comparison of the 9-moment solution (9MA) against the effective static local-field approximation (ESA) (1) data and the 5-moment solution (5MA), i.e. the static approximation for the Nevanlinna function, see Eq. (9), being accurate in the classical limit. The corresponding dynamical structure factor (DSF) from three different models and also the RPA-result is presented in Fig. 1. A systematic analysis is left for a future work, while here we concentrate on the intermediate coupling, $r_s = 2$, where the RPA is already insufficient to accurately reproduce the exchange-correlation effects in the dynamical properties.

First, we observe a very good agreement between the "9MA" and the "ESA". Both independent approaches reproduce a very similar theoretical solution for the DSF, its variation with the wavenumber and even with the temperature varied in the range $1 \leq \theta \leq 4$. The half-width of the DSF around the maximum (the plasmon mode) and the position of the latter demonstrate a remarkable agreement. Some noticeable discrepancies appear only at small wavenumbers (i.e. $k/k_F = 0.60$). However, this result could be expected as the principle of entropy maximization tends to smooth any sharp (resonance) features present in the spectral density.

Both theoretical approximations (ESA and 9MA), where the correlations effects are included via the power moments $C_0(q)$ and $C_4(q)$, significantly deviate from the RPA-result, in particular by lowering the temperature and the wavenumber (see the plots of DSF in Fig. 1 for $q \leq 2.3$ and $\theta \leq 2$). On the other hand, all three theories agree for large wavenumbers ($k/k_F \gtrsim 2.98$) where a broad multiexcitation continuum is present.

Now we turn to the discussion of the DSF in the "classical" limit, see the "5MA"-solution. The term "classical" applies only to the analytical form used for the inverse dielectric function (and the dynamic structure factor) similar to the one considered earlier for the description of the dynamic properties of the classical OCP systems. In contrast, here the power moments C_0, C_4

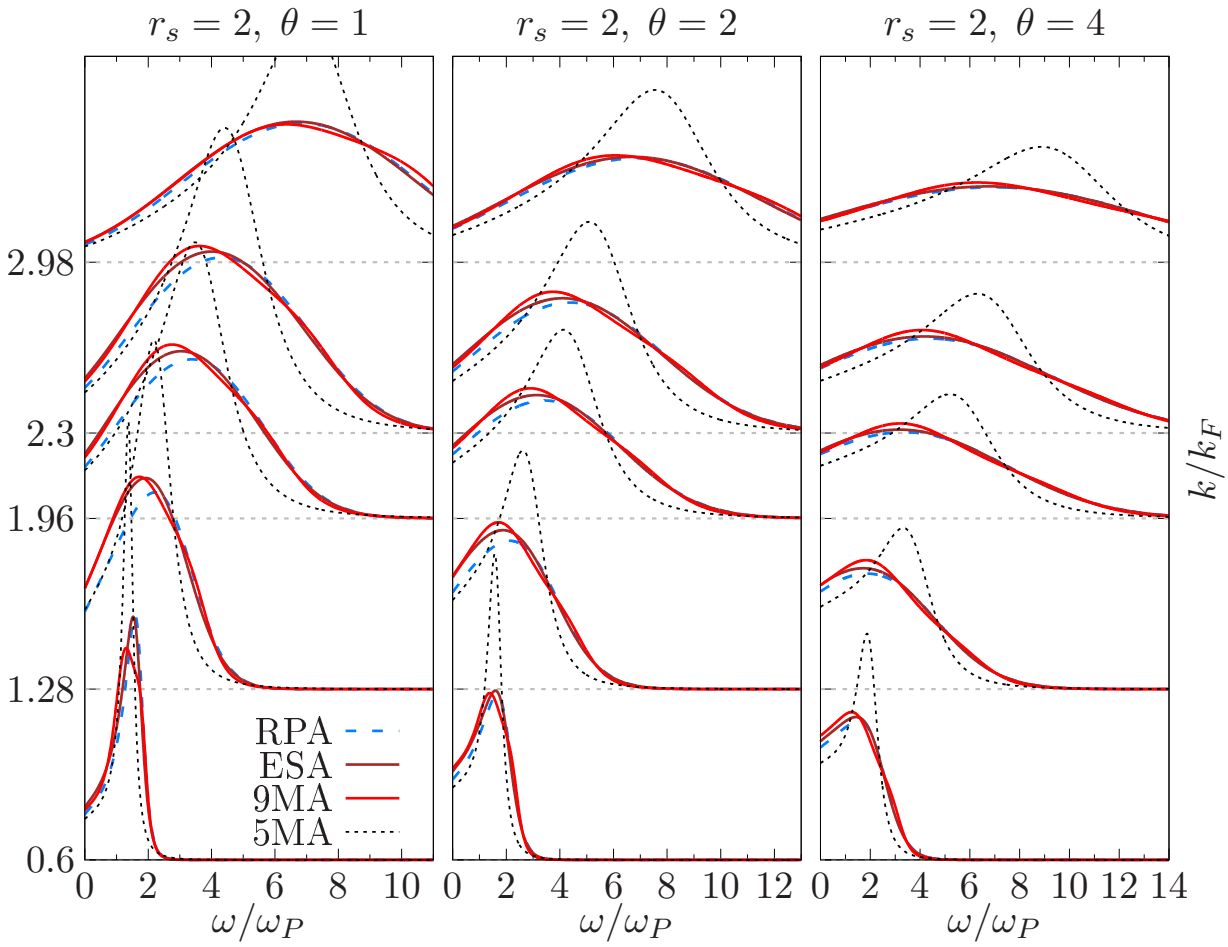

Figure 1. The dynamic structure factor $S(k,\omega)$ at three temperatures $\{\theta = 1, 2, 4\}$ and $r_s = 2.0$. The DSF plots are shifted by the value of k/k_F (horizontal dotted lines). Compared are the results of the random-phase approximation (RPA), the *effective static approximation* (ESA) (1) and the present self-consistent method of moments (SCMM) in the nine-moment ("9MA") and five-moment ("5MA") cases. Note that the five-moment approximation corresponds to the static approximation, Eq. (9), for the Nevanlinna parameter function Q_2. Discrepancies observed for $k/k_F = 0.60$ are due the Shannon entropy maximization which tends to smooth sharp energy resonances and is much better suited for description of a broad multi-excitation continuum. In this case a slight modification of the frequency $\omega_3(k)$ was enough to achieve the level of agreement observed for other wavenumbers.

go beyond the traditional classical description and include the correlation and degeneracy effects via the static structure factor (SSF) provided by the QMC simulations.

For the lowest temperature considered ($\theta = 1$) the 5MA-model provides the correct position of the main plasmon mode, however, it significantly underestimates its broadening due to the damping effects and presence of the second harmonic. The absence of a second harmonic in this solution also at other temperatures ($\theta = 2, 4$) shifts the main peak position in the "5MA"-solution to higher frequencies. Simultaneously, the peak amplitude is reduced and the overall shape approaches that of the 9MA-solution. In the limit of higher temperatures ($\theta \gtrsim 16$) both solutions are excepted to coincide. This gradual transition can be systematically investigated by the analysis of the temperature dependence of the higher-moments (C_6 and C_8) or the frequencies

$\omega_{3(4)}$.

While the high-temperature case is left for the future work, as a preliminary result we demonstrate in Fig. 2 the temperature and the wavenumber dependence of the characteristic frequencies. One can clearly see, that the frequencies $\omega_{3(4)}\,(q)$ grow faster with the temperature in contrast to $\omega_{1(2)}(q)$. As a result, in the limiting case ($\theta \gg 1$) the dynamic frequency-dependent Nevanlinna function (10) should reduce to its static limiting form $ih_2(q;\omega_1,\omega_2)$. In other words, when the system effectively loses its quantum character, we return to the five-moment case which proved to be valid for classical systems.

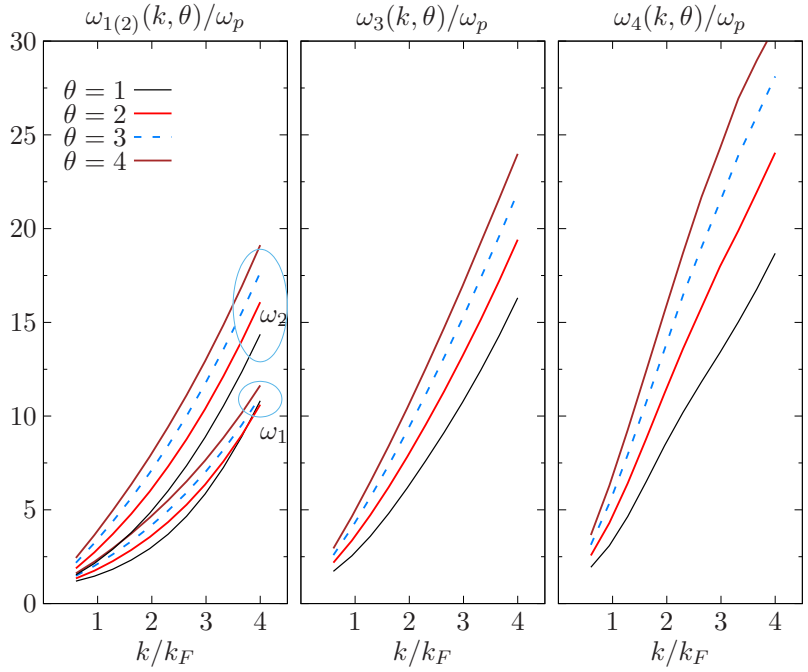

Figure 2. The temperature and wavenumber dependence of the characteristic frequencies $\omega_i\,(i = 1,\ldots 4)$ (in units of plasma frequency) defined via the power moments, see Eq. (4). The frequencies $\omega_{3(4)}$ have been obtained via the Shannon entropy maximization. Simulation parameters: $r_s = 2$ and $\theta = 1, 2, 3, 4$.

Finally, we note that the properties of the collective modes (and the presence of a second harmonic) within our approach can be studied by the solution of the dispersion equation or as the poles of the inverse dielectric function. The corresponding algebraic equation is of the fifth-order and can be written in a closed analytical form. But this analysis goes beyond of the scope of the present short paper.

6. Conclusions

The dynamic structure factor of a warm and dense uniform electron gas is successfully studied within two sequential versions of the self-consistent method of moments based on the exact sum rules, mathematical theorems, and other exact relations. The novel analytical expression for the loss-function is introduced based on the nine-moment approximation and is complemented by the Shannon information entropy maximization technique. As a result, we reduce the knowledge of the dynamic properties of quantum plasmas to the knowledge of a single quantity, i.e. the static structure factor.

Special attention is paid to the temperature dependence and transition between the degenerate ($\theta = 1$) and non-degenerate regime ($\theta = 4$). We demonstrate the superior accuracy and validity of our approach both for low and high temperatures by a direct comparison with the effective static local-field approximation (1) data based on the ab-initio PIMC simulations. For all cases considered both theoretical results are found to be in a nice agreement.

The comparison between the more general 9-moment approximation and the 5-moment solution can be used in the further analysis of the transition from the quantum to classical cases.

We stress that in the 5- and 9-moment calculations the only input was the static structure factor calculated independently using, e.g., the effective static local-field correction (1) or direct quantum Monte-Carlo simulations. The dielectric function we obtain simultaneously can be also used in a variety of problems, see e.g. Ref. (19) and references therein.

6.1. Acknowledgments

A.V. Filinov and I.M. Tkachenko acknowledge support provided by the German Science Foundation (DFG) (grant BO1366-15) and by the Ministry of Education and Science of Kazakhstan (grant AP09260349), respectively.

References

[1] Dornheim T, Cangi A, Ramakrishna K, Böhme M, Tanaka S and Vorberger J 2020 *Phys. Rev. Lett.* **125**(23) 235001 URL https://link.aps.org/doi/10.1103/PhysRevLett.125.235001

[2] Dornheim T, Moldabekov Z A and Vorberger J 2021 *Contributions to Plasma Physics* **61** e202100098

[3] Hamann P, Dornheim T, Vorberger J, Moldabekov Z A and Bonitz M 2020 *Phys. Rev. B* **102**(12) 125150 URL https://link.aps.org/doi/10.1103/PhysRevB.102.125150

[4] Ara J, Coloma L and Tkachenko I 2022 *17th Intl. Conf. on the Physics of Non-Ideal Plasmas, September 20 – 24, 2021, Dresden, Alemania, Book of Abstracts, p. 26*

[5] Ara J, Coloma L and Tkachenko I M 2021 *Physics of Plasmas* **28** 112704 (*Preprint* https://doi.org/10.1063/5.0062259) URL https://doi.org/10.1063/5.0062259

[6] Ara J, Coloma L, Filinov A and Tkachenko I 2022 *42-nd International Workshop on High-Energy-Density Physics with Intense Ion and Laser Beams, Book of abstracts, p. 22*

[7] Arkhipov Y V, Askaruly A, Davletov A E, Dubovtsev D Y, Donkó Z, Hartmann P, Korolov I, Conde L and Tkachenko I M 2017 *Phys. Rev. Lett.* **119**(4) 045001 URL https://link.aps.org/doi/10.1103/PhysRevLett.119.045001

[8] Arkhipov Y V, Ashikbayeva A, Askaruly A, Davletov A E, Dubovtsev D Y, Santybayev K S, Syzganbayeva S A, Conde L and Tkachenko I M 2020 *Phys. Rev. E* **102**(5) 053215 URL https://link.aps.org/doi/10.1103/PhysRevE.102.053215

[9] Dornheim T, Groth S and Bonitz M 2017 *Contributions to Plasma Physics* **57** 468–478

[10] Dornheim T, Groth S and Bonitz M 2018 *Phys. Rep.* **744** 1 – 86 ISSN 0370-1573 URL http://www.sciencedirect.com/science/article/pii/S0370157318300516

[11] Nevanlinna R 1922 *Asymptotische Entwicklungen beschränkter Funktionen und das Stieltjessche Momentenproblem* STK (Helsinki)

[12] Shohat J and Tamarkin J 1943 *The Problem of Moments* Amer. Math. Soc. (Providence, R.I.)

[13] Tkachenko I, Arkhipov Y and Askaruly A 2012 *The Method of Moments and its Applications in Plasma Physics* (Lambert)

[14] Krein M and Nudel'man A 1977 *The Markov moment problem and extremal problems* Trans. of Math. Monographs 50, Amer. Math. Soc. (Providence, R.I.)

[15] Shannon C E 1948 *Bell System Technical Journal* **27** 379–423

[16] Khinchin A 1953 *Uspekhi Mat. Nauk* **8** 3

[17] Zubarev D 1974 *Nonequilibrium Statistical Mechanics* (Consultants Bureau, London)

[18] Jaynes E T 1957 *Phys. Rev.* **106**(4) 620–630 URL https://link.aps.org/doi/10.1103/PhysRev.106.620

[19] Zan X, Lin C, Hou Y and Yuan J 2021 *Phys. Rev. E* **104**(2) 025203 URL https://link.aps.org/doi/10.1103/PhysRevE.104.025203